

pubs.acs.org/JPCA Article

What is the Mechanism of H₃⁺ Formation from Cyclopropane?

Sung Kwon, Shawn Sandhu, Moaid Shaik, Jacob Stamm, Jesse Sandhu, Rituparna Das, Caitlin V. Hetherington, Benjamin G. Levine, and Marcos Dantus*



Cite This: J. Phys. Chem. A 2023, 127, 8633-8638



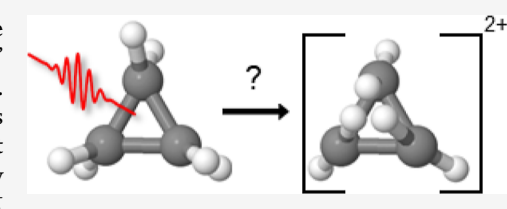
ACCESS I

III Metrics & More

Article Recommendations

Supporting Information

ABSTRACT: We examine the possibility that three hydrogen atoms in one plane of the cyclopropane dication come together in a concerted "ring-closing" mechanism to form H_3^+ , a crucial cation in interstellar gas-phase chemistry. Ultrafast strong-field ionization followed by disruptive probing measurements indicates that the formation time of H_3^+ is 249 ± 16 fs. This time scale is not consistent with a concerted mechanism, but rather a process that is preceded by ring opening. Measurements on propene, an isomer of cyclopropane, reveal the H_3^+



formation time to be 225 ± 13 fs, a time scale similar to the H_3^+ formation time in cyclopropane. Ab initio molecular dynamics simulations and the fact that both dications share a common potential energy surface support the ring-opening mechanism. The reaction mechanism following double ionization of cyclopropane involves ring opening, then H-migration, and roaming of a neutral H_2 molecule, which then abstracts a proton to form H_3^+ . These results further our understanding of complex interstellar chemical reactions and gas-phase reaction dynamics relevant to electron ionization mass spectrometry.

1. INTRODUCTION

Our interest in H_3^+ forming reactions is related to astrochemistry. H_3^+ acts as an interstellar acid in a proton-hop reaction and promotes the formation of water and other small molecules in interstellar space, crucial molecules to initiate star formation. The gas-phase reactivity of this compound is enhanced by the fact that it is triatomic, leaving a third body to carry away the excess energy. As H_3^+ is one of the most abundant triatomic cations in the universe, it is important to understand its formation from various organic molecules upon double ionization because of similarities to its formation as a result of $H_2 + H_2^+$ collisions. Furthermore, small organic molecules have been found to be a minor, but additional source of H_3^+ in the interstellar medium.

Ultrafast dissociative ionization methods allow researchers to explore the mechanism of formation of fragment ions, including H_3^+ , by irradiating molecules with powerful femtosecond laser pulses. ^{6–8} It must be noted that the unimolecular reaction that leads to H_3^+ formation requires the breaking of three bonds and formation of three new H–H bonds, which often involves significant deformation of the molecular geometry. Therefore, studying the mechanism of H_3^+ formation from ionized hydrocarbons deepens our understanding of such complex ultrafast molecular dynamics and inspires approaches to control them. ^{9–12}

 $\mathrm{H_3^+}$ has been observed from the fragmentation of doubly ionized molecules. The $\mathrm{H_{3^+}}$ formation reaction in ethane involves hydrogen migration, and theory indicates a transition state in which $\mathrm{H_2}$ is attached to the remaining dication. Another mechanism, known as roaming, is observed in alcohols and other small organic molecules. In this mechanism, upon double ionization, two hydrogen atoms

combine to form $\rm H_2$ which then undergoes roaming in proximity to the dication before eventually abstracting a proton to form. $^{7,8,17-19}$

The dissociative double photoionization of cyclopropane has been examined previously in the 25-35 eV photon range.²⁰ In that study, which included ab initio calculations at the level CASSCF/CASPT2 theory and cc-pVTZ basis-set, the double ionization potential was calculated to be 31.28 eV, and the appearance energy for the following doubly charged species was determined to be $C_3H_2^{2+}$ (34.0 eV), $C_3H_3^{2+}$ (35.0 eV), $C_3H_4^{2+}$ (30.5 eV), and $C_3H_5^{2+}$ (33.0 eV). It was found that several dissociation channels appeared below the double ionization potential, indicating that Jahn-Teller distortion led to symmetry breaking. The extent of ring deformation and H-evaporation populates different dication states, which act as gateway states for different dissociation channels. Ring opening was associated with C3H42+ and ring closing was associated with C₃H₅²⁺. Furthermore, Oghbaie et al. proposed a novel ring-closing mechanism for the formation of H₃⁺ that preserves the D_{3h} symmetry upon double ionization and involves the simultaneous dissociation of three C–H bonds, 20 as shown in Figure 1. We were intrigued by their proposal of a new H₃⁺ formation mechanism and embarked on the present study.

Received: August 11, 2023 Revised: September 21, 2023 Published: October 9, 2023





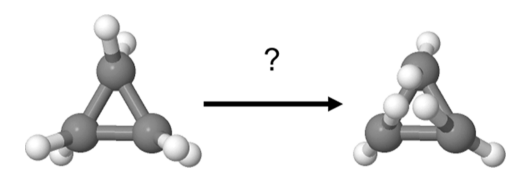


Figure 1. Proposed ring-closing mechanism, where three hydrogens come together on the same plane of doubly ionized cyclopropane. Jmol software was used to make this figure.²¹

2. METHODS

The experimental methodology used here to track multiple reaction pathways following ultrafast ionization, has been described in detail elsewhere. In short, a Ti:sapphire laser producing 35 fs pulses with a central wavelength of 800 nm was used as the ionization source. The pulses were compressed using the multiphoton intrapulse interference phase scan method, which measures and compresses the pulses using a pulse shaper. The laser pulses were focused inside a Wiley–McLaren time-of-flight (TOF) mass spectrometer via a concave gold-coated mirror. Each pulse was split into a strong pump (5.5 \times 10¹⁴ W/cm²), which causes tunnel ionization, and a weak probe (9.5 \times 10¹³ W/cm²), which disrupts product formation. The laser intensities were calibrated by measuring the ratio between Ar $^+$ and Ar $^{2+}$ ions.

Given the ionization potentials of cyclopropane and propene (9.90 and 9.73 eV, respectively),²⁵ the intensity of the pump yielded Keldysh parameters of 0.39 for both compounds,² indicating that ionization occurs within an optical cycle via tunnel ionization. The cyclopropane and propene gases were introduced to the TOF chamber via an effusive beam through a needle valve. The static pressure inside the vacuum chamber during data acquisition was maintained at 7×10^{-6} Torr. The baseline vacuum pressure was 9×10^{-8} Torr, and when the needle valve was closed, the pressure returned to baseline within seconds, ensuring fast sample refresh. The ion signals were digitized using an oscilloscope (LeCroy WaveRunner 610Zi, 1 GHz). For H₃⁺ time-resolved data, a -125 V bias in the X direction was applied by using a pair of plates located before the field-free region of the TOF to avoid saturation of peaks with relatively large m/z ratios. The TOF was configured to measure positive ions, therefore, only cationic peaks are shown in the mass spectra.

To gain further insight into the mechanistic details of H₃⁺ formation in cyclopropane, we conducted ab initio molecular dynamics (AIMD) using the GPU-accelerated electronic structure package TeraChem. ^{27–29} All trajectories were carried out using B3LYP/aug-cc-pVDZ with a velocity Verlet integrator with a time step of 0.5 fs and integrated for up to 750 fs. A total of 500 trajectories were computed for each molecule. For all trajectories, the initial position and momentum were sampled from the neutral ground state Wigner distribution using the aforementioned level of theory. Trajectories were initiated on the dication ground state potential energy surface (PES), assuming vertical excitation of the neutral. All trajectories and molecular geometries were visualized using Avogadro. 30,31 Using TeraChem, the geometries (both minima and transition states) for the potential energy curve were calculated using B3LYP/aug-cc-pVDZ. The single-point energies were determined using CCSD(T)/augcc-pVDZ implemented in GAMESS.32-34 We found good agreement (differences <0.25 eV) between the energies calculated by both methods.

3. RESULTS AND DISCUSSION

The experimental strong-field ionization (SFI) mass spectra of cyclopropane and propene are shown in Figure 2. We found

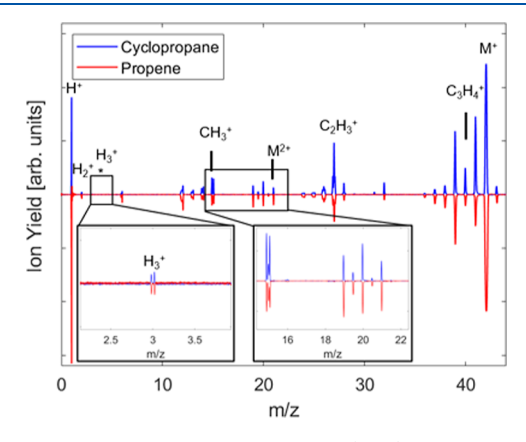


Figure 2. SFI mass spectra of cyclopropane (blue) and propene (red). The single pulse intensity for ionization was $5.5 \times 10^{14} \text{ W/cm}^2$. Each spectrum was normalized by dividing the amplitude by the sum of all peak areas. The left inset shows a zoomed-in region of the spectra where the H_3^+ is observed. The inset on the right shows the CH_3^+ and $C_3H_n^{2+}$ fragments.

both SFI spectra to be very similar. The peak at m/z 15 corresponds to $\mathrm{CH_3}^+$ in both compounds, which suggests that hydrogen migration occurs in cyclopropane. In fact, the $\mathrm{CH_3}^+$ yield is greater for cyclopropane. In addition, we observe that for the dication fragments, loss of two hydrogens occurs with greater probability than loss of individual hydrogen atoms. This likely implies that loss of neutral $\mathrm{H_2}$ from both compounds is favored over loss of individual hydrogen atoms.

We compare the SFI spectrum obtained with that obtained by Oghbaie et al. 20 to ensure similar internal energies, allowing us to evaluate if the formation of ${\rm H_3}^+$ follows their suggested ring-closing mechanism. This determination is done by matching the abundance of "thermometer ions". The SFI spectrum of cyclopropane is in very close agreement with the single 35 eV photoionization of cyclopropane, as determined by the similar relative ion yields for all m/z values. This indicates that the SFI process leads to a vertical ionization energy similar to that of the 35 eV photoionization. Further evidence of the internal energy acquired by the molecules during SFI comes from the observation of ${\rm H_3}^+$ and ${\rm C_3H_3}^{2+}$, which have appearance energies of 32.5 and 35.0 eV, respectively. 20

The H₃⁺ ion appears as a doublet in the TOF spectrum as a result of the Coulomb repulsion between H₃⁺ and the counterion. The forward and backward ejections along the TOF lead to different times of arrival, which can be used to determine the kinetic energy release (KER) of this fragment (Figure S1). The H₃⁺ doublet was integrated as a function of the delay between the pump and probe pulses. The timeresolved dynamics of H₃⁺ from cyclopropane and propene is shown in Figure 3. The positive feature at zero delay between pump and probe pulses is caused by the increased intensity of the time-overlapped pulses, which causes a greater ion yield as their intensities sum when overlapped in time. The depletion that follows is caused by the probe pulse disrupting the formation of H₃⁺ by shifting the branching ratio to a different reaction pathway. By tracking the decay and recovery, we can determine the time scale of formation for all ions in the mass

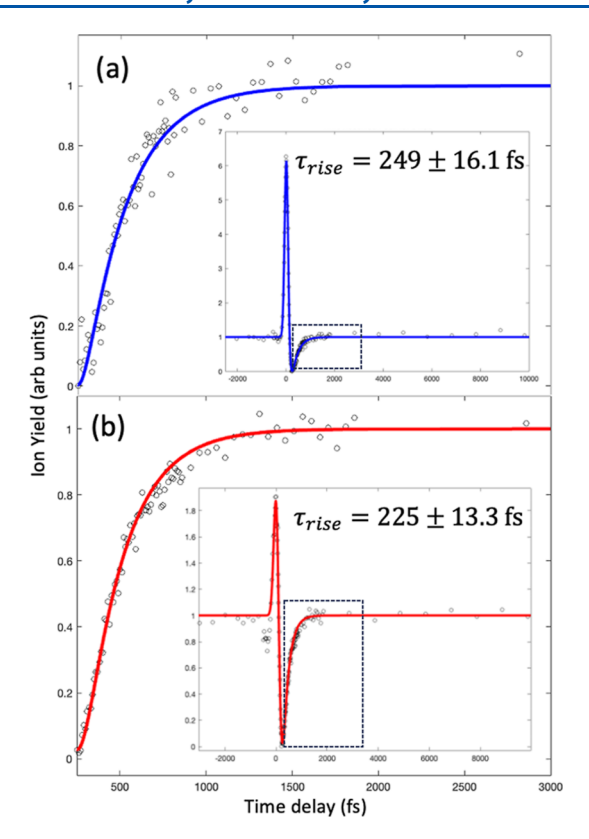


Figure 3. Time-resolved fitted H_3^+ ion formation from (a) cyclopropane and (b) propene based on the pump-probe delay is shown in figure. The circles correspond to experimental data. The blue and red lines indicate the exponential fit corresponding to eq 2.

spectrum, including H_3^+ . The entire experimental transient can be fit to the function

$$P(t, \tau_1, \tau_2) = ae^{-t^2/s^2} + bP_1(t, \tau_1) + cP_2(t, \tau_2)$$
 (1)

where

$$P_i(t, \tau_i) = e^{-t/\tau_i} \left(1 + \operatorname{erf}\left(\frac{t}{s} - \frac{s}{2\tau_i}\right) \right)$$
(2)

For the abovementioned equation, a, b, and c are the amplitude factors, τ_i is a time constant defining a decay ($\tau_{\rm decay}$) or rise ($\tau_{\rm rise}$) of the signal, t is a specific pump-probe delay, and s is a parameter related to the full width at half max (fwhm) of the pulse duration by

$$\tau_{\text{FWHM}} = 2\sqrt{\ln 2} \cdot s \tag{3}$$

The specific fitting parameters used can be found in the Supporting Information.

The time scale of formation of H_3^+ is obtained by fitting the experimental data using eq 2 and are found to be $\tau = 249 \pm 16$ fs and $\tau = 225 \pm 13$ fs for cyclopropane and propene, respectively.

To gain insight into the reaction mechanism, we performed AIMD trajectories on the dication states of cyclopropane and propene. In Figure 4, we show a representative trajectory for cyclopropane where ring-opening occurs within the first 29 fs. This is followed by H migration, the formation of neutral H_2 , which roams near the dication, and finally the abstraction of a proton to form H_3^+ (see Video S1).

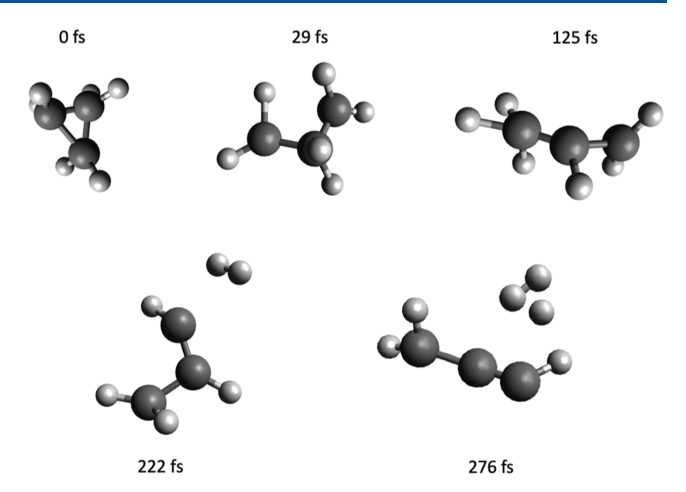


Figure 4. AIMD trajectory of ${\rm H_3}^+$ formation via hydrogen migration and ${\rm H_2}$ roaming. Snapshots were taken from the cyclopropane trajectory shown in Video S1. The trajectory was calculated by using B3LYP/aug-cc-pVDZ.

We find that some reaction pathways that lead to the formation of H_3^+ for both molecules share the same intermediates and transition states (Figure 5 and Video S1). For both molecules, the dication minimum is identical (Figure 5) with equal positive charge densities on both carbon ends (Figure S2). From 500 AIMD trajectories for each compound, 10 and 9 trajectories for cyclopropane and propene, respectively, resulted in H_3^+ formation. All 500 trajectories for cyclopropane showed ring opening occurring within 30 fs of double ionization. The average time scale of the trajectories forming H_3^+ was 281 and 271 fs for cyclopropane and propene, respectively. These values are in close agreement with our experimental measurements.

The similarities in H_3^+ formation time scales support the ring-opening mechanism in cyclopropane. Moreover, these time scales show that the slightly longer H_3^+ formation time for cyclopropane is partially due to the time for ring opening.

We find the relatively long time scale of the H₃⁺ formation and the AIMD trajectories to be inconsistent with the ringclosing mechanism proposed by Oghbaie et al.²⁰ One would expect the ring-closing mechanism, which involves the concerted coalescence of three hydrogen atoms on the same plane of cyclopropane, to occur in a single kinetic step on a time scale of a few hydrogen-puckering vibrational periods (the symmetric ν_3 mode, 851 cm⁻¹, B3LYP/aug-cc-pVDZ, ~39 fs period). Thus, we propose that the dominant mechanism of H₃⁺ formation is the ring-opening mechanism. This is additionally supported by the SFI spectrum, as well as the photoionization spectrum,²⁰ which show a 4-6 times greater yield for C₃H₄²⁺ fragment (associated with ring opening) than C₃H₅²⁺ fragment (associated with ring closing). Also, the similarity found in the KER analysis of the H₃⁺ peaks for both compounds provides further evidence for the ring-opening mechanism (Figure S1).

Having identified the ring-opening mechanism identified, high-level quantum chemical calculations were used to quantify the associated energetics. Several intermediate structures common to cyclopropane and propene are observed prior to the formation of H_3^+ as seen in Figure 5. We found that the density functional theory PES used in the AIMD trajectories is in very good agreement with the energies computed at the CCSD(T) level (Figure 5). The positive charges on both

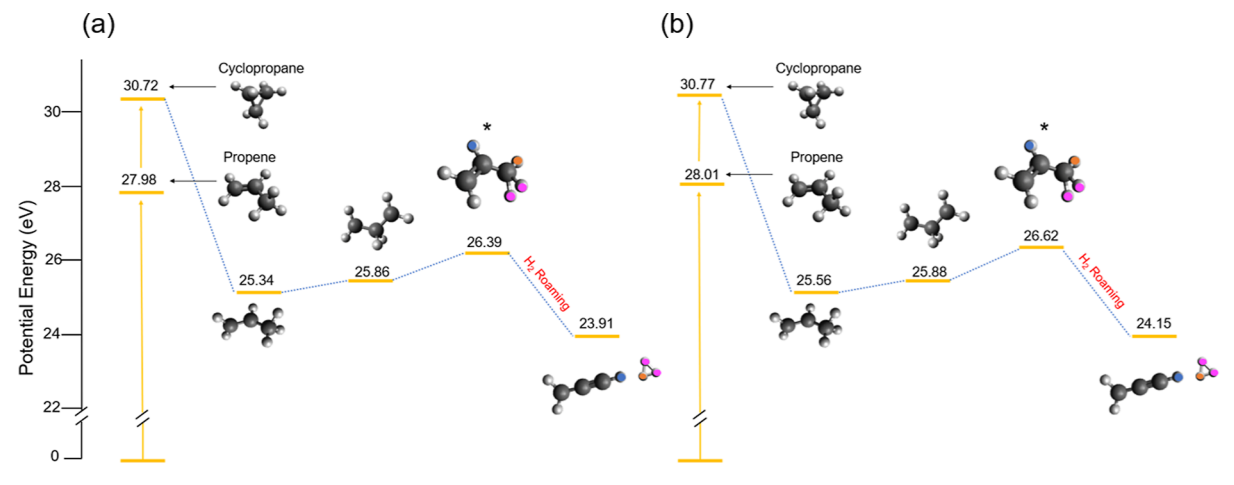


Figure 5. Potential energy diagram for cyclopropane and propene depicting the formation of H_3^+ . The geometries were optimized using B3LYP/aug-cc-pVDZ, and the energies were calculated for (a) using CCSD(T)/aug-cc-pVDZ and for (b) using B3LYP/aug-cc-pVDZ. Transition states are denoted by asterisks next to the structure. Initially, one hydrogen atom migrates from the middle carbon (colored orange) to join the two other hydrogen atoms on a terminal carbon (colored pink); this step is followed by formation of neutral H_2 , and upon proton abstraction, the remaining H atom (colored blue) in the central carbon migrates to the end carbon.

carbon ends pull electron density away from the secondary carbon, weakening its C-H bonds (Figure S2). This is a key step prior to hydrogen migration and formation of H_2 . The excess energy following double ionization provides the driving force, which allows for bond cleavage and rearrangements.

In all observed trajectories in which H_3^+ was formed, we noticed that after hydrogen migration, neutral H_2 roamed near the dication before abstracting a proton (see supplementary Video S1 for a representative trajectory of H_3^+ formation from cyclopropane and propene). Overall, our experimental and theoretical work provides compelling evidence that ring-opening occurs after the double ionization of cyclopropane. It remains to be explored if SFI with a laser pulse duration shorter than the 20 fs associated with Jahn–Teller distortion can cause ultrafast excitation to a different electronic state of the dication that will result in the ring-closing mechanism of H_3^+ formation.

4. CONCLUSIONS

We determined the dominant mechanism of H_3^+ formation from doubly ionized cyclopropane to be ring opening, followed by hydrogen migration, formation of neutral H_2 , roaming, and proton abstraction to form H_3^+ . This conclusion is supported by experimental ultrafast dynamics, ab initio molecular dynamics, and ab initio electronic structure calculations. The experimental H_3^+ formation time scale from cyclopropane is 249 fs and provides compelling evidence for the proposed ring-opening mechanism, rather than the ring-closing mechanism previously suggested in the literature. Furthermore, doubly ionized propene was observed to form H_3^+ in 225 fs, a time scale close to the formation of H_3^+ from cyclopropane. The findings presented in this study contribute to our understanding of gas-phase chemistry and complex dynamics following the ionization of organic molecules leading to H_3^+ .

ASSOCIATED CONTENT

Supporting Information

The Supporting Information is available free of charge at https://pubs.acs.org/doi/10.1021/acs.jpca.3c05442.

AIMD trajectories showing H migration, the formation of neutral H_2 , and the abstraction of a proton to form H_3^+ for both cyclopropane and propene (MP4)

Reagents, fitting equation parameters, experimental analysis including kinetic energy release, and theoretical analysis including the Mulliken charges for the common dication minimum for cyclopropane and propene (PDF)

AUTHOR INFORMATION

Corresponding Author

Marcos Dantus — Department of Chemistry and Department of Physics and Astronomy, Michigan State University, East Lansing, Michigan 48824, United States; orcid.org/0000-0003-4151-5441; Email: dantus@chemistry.msu.edu

Authors

Sung Kwon – Department of Chemistry, Michigan State University, East Lansing, Michigan 48824, United States Shawn Sandhu – Department of Chemistry, Michigan State University, East Lansing, Michigan 48824, United States; orcid.org/0000-0001-6252-4270

Moaid Shaik — Department of Chemistry, Michigan State
University, East Lansing, Michigan 48824, United States
Jacob Stamm — Department of Chemistry, Michigan State
University, East Lansing, Michigan 48824, United States
Jesse Sandhu — Department of Chemistry, Michigan State
University, East Lansing, Michigan 48824, United States
Rituparna Das — Department of Chemistry, Michigan State
University, East Lansing, Michigan 48824, United States
Caitlin V. Hetherington — Department of Chemistry and
Institute of Advanced Computational Science, Stony Brook
University, Stony Brook, New York 11794, United States;
orcid.org/0000-0003-1839-2500

Benjamin G. Levine – Department of Chemistry and Institute of Advanced Computational Science, Stony Brook University, Stony Brook, New York 11794, United States; orcid.org/0000-0002-0356-0738

Complete contact information is available at: https://pubs.acs.org/10.1021/acs.jpca.3c05442

Notes

The authors declare no competing financial interest.

ACKNOWLEDGMENTS

This material is based on the work supported by the Department of Energy, Office of Basic Energy Sciences, Atomic, Molecular, and Optical Sciences Program under award number SISGR (DE-SC0002325). R.D. was funded by the Air Force Office of Scientific Research under award number FA9550-21-1-0428. This work used the SDSC Expanse GPU at San Diego Supercomputer Center through allocation CHE230046 from the Advanced Cyberinfrastructure Coordination Ecosystem: Services & Support (ACCESS) program, which is supported by National Science Foundation grants #2138259, #2138286, #2138307, #2137603, and #2138296. B.G.L. gratefully acknowledges support from the National Science Foundation CHE-1954519.

REFERENCES

- (1) Watson, W. D. The rate of formation of interstellar molecules by ion—molecule reactions. *Astrophys. J.* **1973**, *183*, L17.
- (2) Oka, T. Interstellar H 3+. Chem. Rev. 2013, 113, 8738-8761.
- (3) Zhou, L.; Ni, H.; Jiang, Z.; Qiang, J.; Jiang, W.; Zhang, W.; Lu, P.; Wen, J.; Lin, K.; Zhu, M.; et al. Ultrafast formation dynamics of D 3⁺from the light-driven bimolecular reaction of the D_2 – D_2 dimer. *Nat. Chem.* **2023**, *15*, 1229–1235.
- (4) Mi, Y.; Wang, E.; Dube, Z.; Wang, T.; Naumov, A.; Villeneuve, D.; Corkum, P.; Staudte, A. D3+ formation through photoionization of the molecular D2-D2 dimer. *Nat. Chem.* **2023**, *15*, 1224–1228.
- (5) Pilling, S.; Andrade, D.; Neves, R.; Ferreira-Rodrigues, A.; Santos, A.; Boechat-Roberty, H. Production of H+3 via photodissociation of organic molecules in interstellar clouds: H+3 photoproduction in interstellar clouds. *Mon. Not. R. Astron. Soc.* **2007**, 375, 1488–1494.
- (6) Kotsina, N.; Kaziannis, S.; Kosmidis, C. Hydrogen migration in methanol studied under asymmetric fs laser irradiation. *Chem. Phys. Lett.* **2014**, *604*, 27–32.
- (7) Ekanayake, N.; Nairat, M.; Kaderiya, B.; Feizollah, P.; Jochim, B.; Severt, T.; Berry, B.; Pandiri, K. R.; Carnes, K. D.; Pathak, S.; et al. Mechanisms and time-resolved dynamics for trihydrogen cation H3⁺formation from organic molecules in strong laser fields. *Sci. Rep.* **2017**, *7*, 4703.
- (8) Ekanayake, N.; Severt, T.; Nairat, M.; Weingartz, N. P.; Farris, B. M.; Kaderiya, B.; Feizollah, P.; Jochim, B.; Ziaee, F.; Borne, K.; et al. H₂ roaming chemistry and the formation of H3⁺from organic molecules in strong laser fields. *Nat. Commun.* **2018**, *9*, 5186.
- (9) Kaziannis, S.; Kotsina, N.; Kosmidis, C. Interaction of toluene with two-color asymmetric laser fields: Controlling the directional emission of molecular hydrogen fragments. *J. Chem. Phys.* **2014**, *141*, 104319.
- (10) Michie, M. J.; Ekanayake, N.; Weingartz, N. P.; Stamm, J.; Dantus, M. Quantum coherent control of h 3⁺formation in strong fields. *J. Chem. Phys.* **2019**, *150*, 044303.
- (11) Iwamoto, N.; Schwartz, C. J.; Jochim, B.; Raju P, K.; Feizollah, P.; Napierala, J.; Severt, T.; Tegegn, S.; Solomon, A.; Zhao, S.; et al. Strong-field control of H3⁺production from methanol dications: Selecting between local and extended formation mechanisms. *J. Chem. Phys.* **2020**, *152*, 054302.
- (12) Townsend, T.; Schwartz, C. J.; Jochim, B.; Raju P, K.; Severt, T.; Iwamoto, N.; Napierala, J.; Feizollah, P.; Tegegn, S.; Solomon, A.; et al. Controlling H3⁺formation from ethane using shaped ultrafast laser pulses. *Front. Phys.* **2021**, *9*, 691727.
- (13) De, S.; Rajput, J.; Roy, A.; Ghosh, P.; Safvan, C. Formation of H3⁺due to intramolecular bond rearrangement in doubly charged methanol. *Phys. Rev. Lett.* **2006**, *97*, 213201.

- (14) Hoshina, K.; Furukawa, Y.; Okino, T.; Yamanouchi, K. Efficient ejection of H3⁺from hydrocarbon molecules induced by ultrashort intense laser fields. *J. Chem. Phys.* **2008**, *129*, 104302.
- (15) Kraus, P. M.; Schwarzer, M. C.; Schirmel, N.; Urbasch, G.; Frenking, G.; Weitzel, K.-M. Unusual mechanism for H3⁺formation from ethane as obtained by femtosecond laser pulse ionization and quantum chemical calculations. *J. Chem. Phys.* **2011**, *134*, 114302.
- (16) Ando, T.; Shimamoto, A.; Miura, S.; Iwasaki, A.; Nakai, K.; Yamanouchi, K. Coherent vibrations in methanol cation probed by periodic H3⁺ejection after double ionization. *Commun. Chem.* **2018**, *1*, 7
- (17) Nakai, K.; Kato, T.; Kono, H.; Yamanouchi, K. Communication: Long-lived neutral H_2 in hydrogen migration within methanol dication. J. Chem. Phys. **2013**, 139, 181103.
- (18) Livshits, E.; Luzon, I.; Gope, K.; Baer, R.; Strasser, D. Timeresolving the ultrafast H₂ roaming chemistry and H3⁺formation using extreme-ultraviolet pulses. *Nat. Comm. Chem.* **2020**, 3, 49.
- (19) Wang, E.; Shan, X.; Chen, L.; Pfeifer, T.; Chen, X.; Ren, X.; Dorn, A. Ultrafast proton transfer dynamics on the repulsive potential of the ethanol dication: Roaming-mediated isomerization versus coulomb explosion. *J. Chem. Phys. A* **2020**, *124*, 2785–2791.
- (20) Oghbaie, S.; Gisselbrecht, M.; Månsson, E. P.; Laksman, J.; Stråhlman, C.; Sankari, A.; Sorensen, S. L. Dissociation of cyclopropane in double ionization continuum. *Phys. Chem. Chem. Phys.* **2017**, *19*, 19631–19639.
- (21) Jmol: an open-source java viewer for chemical structures in 3d. version 14.6.4. 2023, Http://avogadro.ccweb/ (accessed Oct 8, 2023).
- (22) Jochim, B.; DeJesus, L.; Dantus, M. Ultrafast disruptive probing: simultaneously keeping track of tens of reaction pathways. *Rev. Sci. Instrum.* **2022**, *93*, 033003.
- (23) Xu, B.; Gunn, J. M.; Cruz, J. M. D.; Lozovoy, V. V.; Dantus, M. Quantitative investigation of the multiphoton intrapulse interference phase scan method for simultaneous phase measurement and compensation of femtosecond laser pulses. *J. Opt. Soc. Am. B* **2006**, 23, 750–759.
- (24) Guo, C.; Li, M.; Nibarger, J. P.; Gibson, G. N. Single and double ionization of diatomic molecules in strong laser fields. *Phys. Rev. A: At., Mol., Opt. Phys.* **1998**, 58, R4271–R4274.
- (25) Traeger, J. C. A study of the allyl cation thermochemistry by photoionization mass spectrometry. *Int. J. Mass Spectrom. Ion Process.* **1984**, *58*, 259–271.
- (26) Keldysh, L. Ionization in the field of a strong electromagnetic wave. J. Exp. Theor. Phys. 1965, 20, 1307–1314.
- (27) Ufimtsev, I. S.; Martinez, T. J. Quantum chemistry on graphical processing units. 1. strategies for two-electron integral evaluation. *J. Chem. Theory Comput.* **2008**, *4*, 222–231.
- (28) Ufimtsev, I. S.; Martinez, T. J. Quantum chemistry on graphical processing units. 2. direct self-consistent-field implementation. *J. Chem. Theory Comput.* **2009**, *5*, 1004–1015.
- (29) Ufimtsev, I. S.; Martinez, T. J. Quantum chemistry on graphical processing units. 3. analytical energy gradients, geometry optimization, and first principles molecular dynamics. *J. Chem. Theory Comput.* **2009**, *5*, 2619–2628.
- (30) Avogadro: An open-source molecular builder and visualization tool. version 1.2.0. 2023, http://avogadro.ccweb/ (accessed March 8, 2023).
- (31) Hanwell, M. D.; Curtis, D. E.; Lonie, D. C.; Vandermeersch, T.; Zurek, E.; Hutchison, G. R. Avogadro: an advanced semantic chemical editor, visualization, and analysis platform. *J. Cheminf.* **2012**, *4*, 17.
- (32) Schmidt, M. W.; Baldridge, K. K.; Boatz, J. A.; Elbert, S. T.; Gordon, M. S.; Jensen, J. H.; Koseki, S.; Matsunaga, N.; Nguyen, K. A.; Su, S.; et al. General atomic and molecular electronic structure system. *J. Comput. Chem.* **1993**, *14*, 1347–1363.
- (33) Piecuch, P.; Kucharski, S. A.; Kowalski, K.; Musiał, M. Efficient computer implementation of the renormalized coupled-cluster methods: the r-ccsd [t], r-ccsd (t), cr-ccsd [t], and cr-ccsd (t) approaches. *Comput. Phys. Commun.* **2002**, *149*, 71–96.

- (34) Barca, G. M.; Bertoni, C.; Carrington, L.; Datta, D.; De Silva, N.; Deustua, J. E.; Fedorov, D. G.; Gour, J. R.; Gunina, A. O.; Guidez, E.; et al. Recent developments in the general atomic and molecular electronic structure system. *J. Chem. Phys.* **2020**, *152*, 154102.
- (35) Barylyuk, K. V.; Chingin, K.; Balabin, R. M.; Zenobi, R. Fragmentation of benzylpyridinium "thermometer" ions and its effect on the accuracy of internal energy calibration. *J. Am. Chem. Soc.* **2010**, 21, 172–177.